Fig. 1

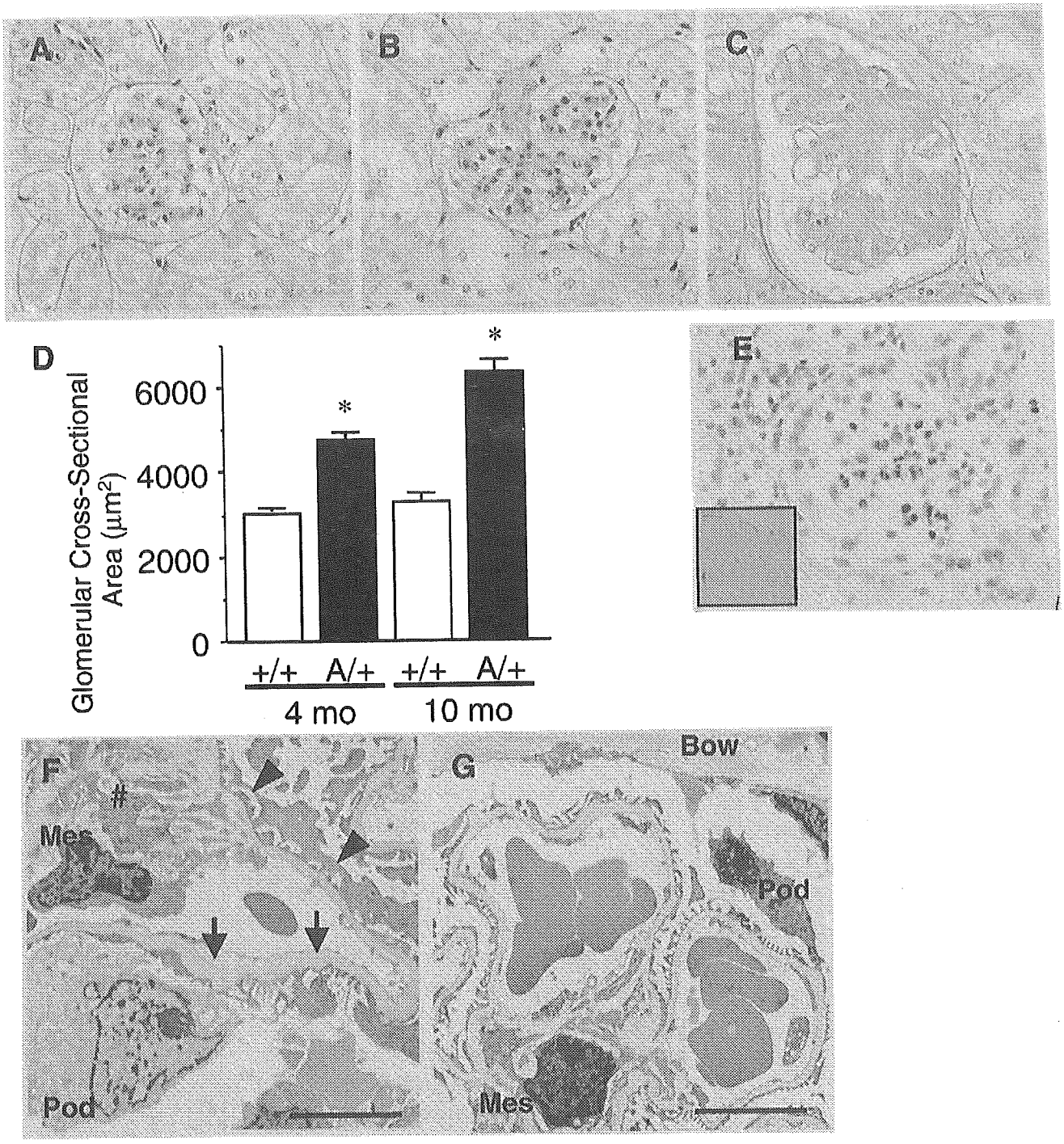

Figure 1. Histological analysis of the kidney in A-ZIP/F-1 mice (A-ZIPTg/+) and wild-type mice (+/+). *A–C*) The kidney sections were stained with periodic acid-Schiff, ×400. A-ZIPTg/+ exhibited marked glomerular hypertrophy and mesangial expansion at 4 months of age (*B*), and these changes were more pronounced at 10 months of age (*C*) as compared with +/+ (*A*). *D*) Quantitative analysis showed glomerular hypertrophy in A-ZIPTg/+. $*P < 0.01$, $n = 6–7$. *E*) Oil Red O staining showed no apparent macrolipid deposits in the kidney of A-ZIPTg/+. (Inset) A positive control of Oil Red O staining in the adipose tissue. Electron microscopy of A-ZIPTg/+ (*F*) and +/+ (*G*). A-ZIPTg/+ showed diffuse thickening of glomerular basement membrane (arrows), foot process effacement of podocytes (arrowheads), and marked expansion of mesangial matrix (#). Mes, mesangial cell; Pod, podocyte; Bow, Bowman's capsule. Scale bar indicates 5 μm.

Fig. 2

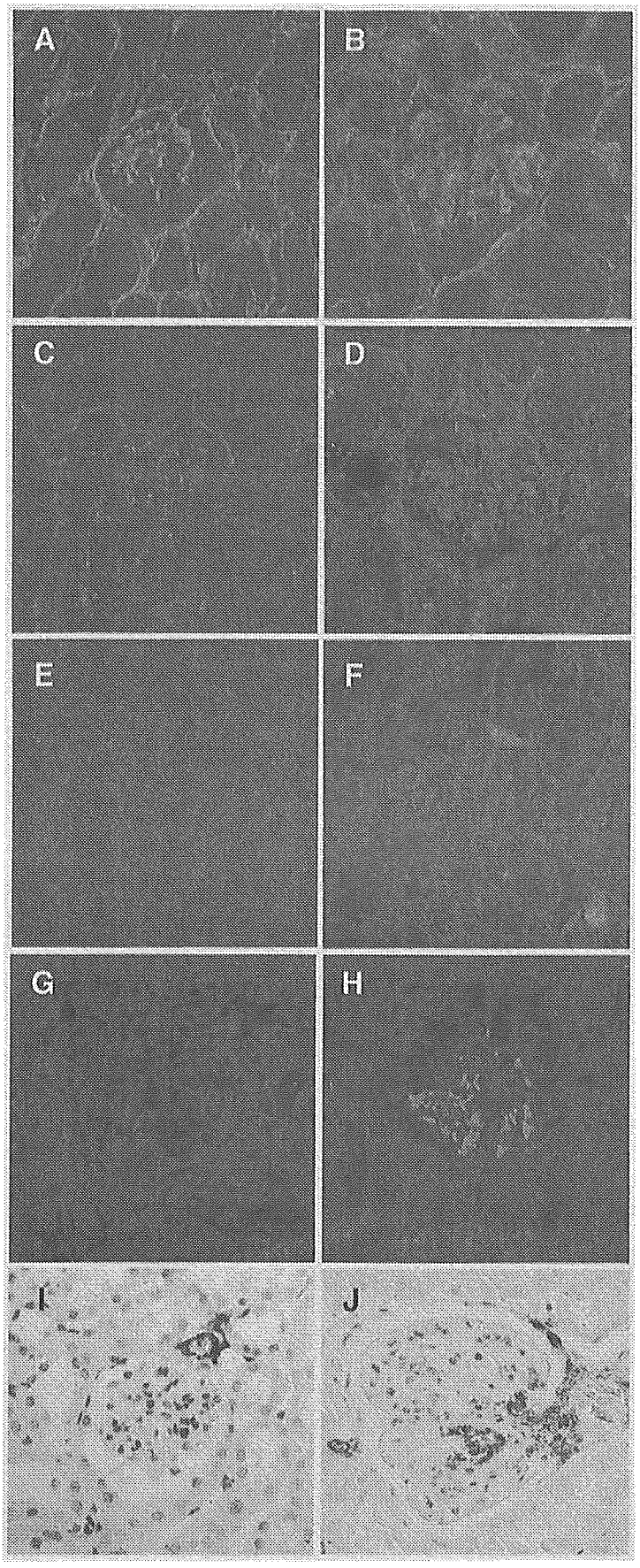

Figure 2. Immunohistochemical analysis for extracellular matrix proteins (collagen type IV (*A*) and (*B*); fibronectin (*C*) and (*D*); collagen type I (*E*) and (*F*), transforming growth factor-β1 (TGF-β1 (*G*) and (*H*)) and α-smooth muscle actin (αSMA, *I* and *J*) in the kidneys from 10-month-old A-ZIPTg/+ (*B*, *D*, *F*, *H*, and *J*) and +/+ (*A*, *C*, *E*, *G*, and *I*). A-ZIPTg/+ showed increased staining of extracellular matrix proteins, TGF-β1, and αSMA in the mesangial area, as compared with +/+ (×400).

Fig. 3

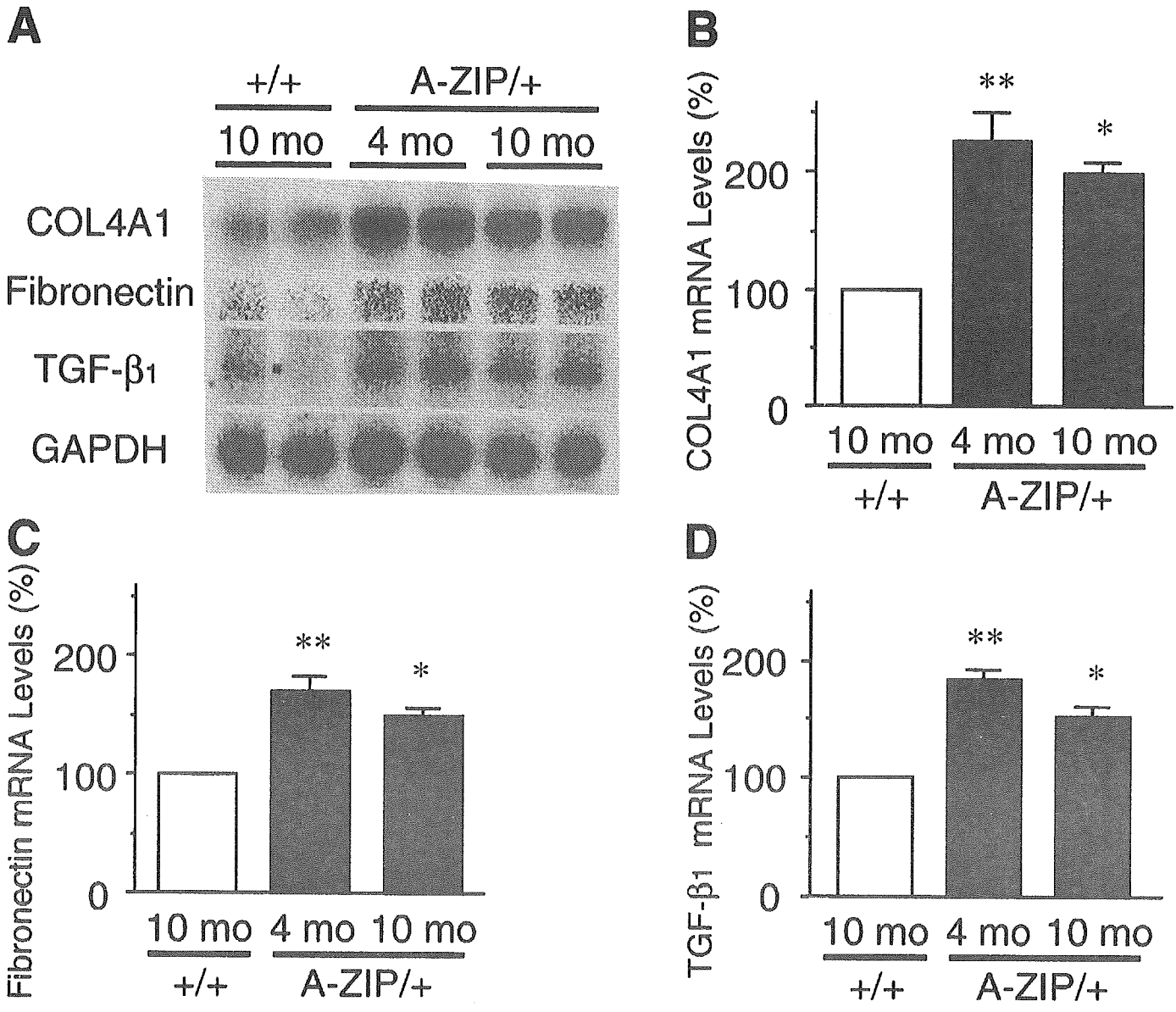

Figure 3. Renal gene expression of collagen type IV α1 chain (COL4A1), fibronectin, and TGF-β1 in A-ZIPTg/+ and +/+. Representative Northern blots (*A*) and quantitative relative mRNA levels (*B–D*) are shown. A-ZIPTg/+ exhibited significant up-regulation of COL4A1, fibronectin, and TGF-β1 mRNAs from 4 months of age as compared with +/+. Mean ± SE. $*P < 0.05$, $**P < 0.01$ vs. 10-month-old +/+, $n = 6–8$.

Fig. 4

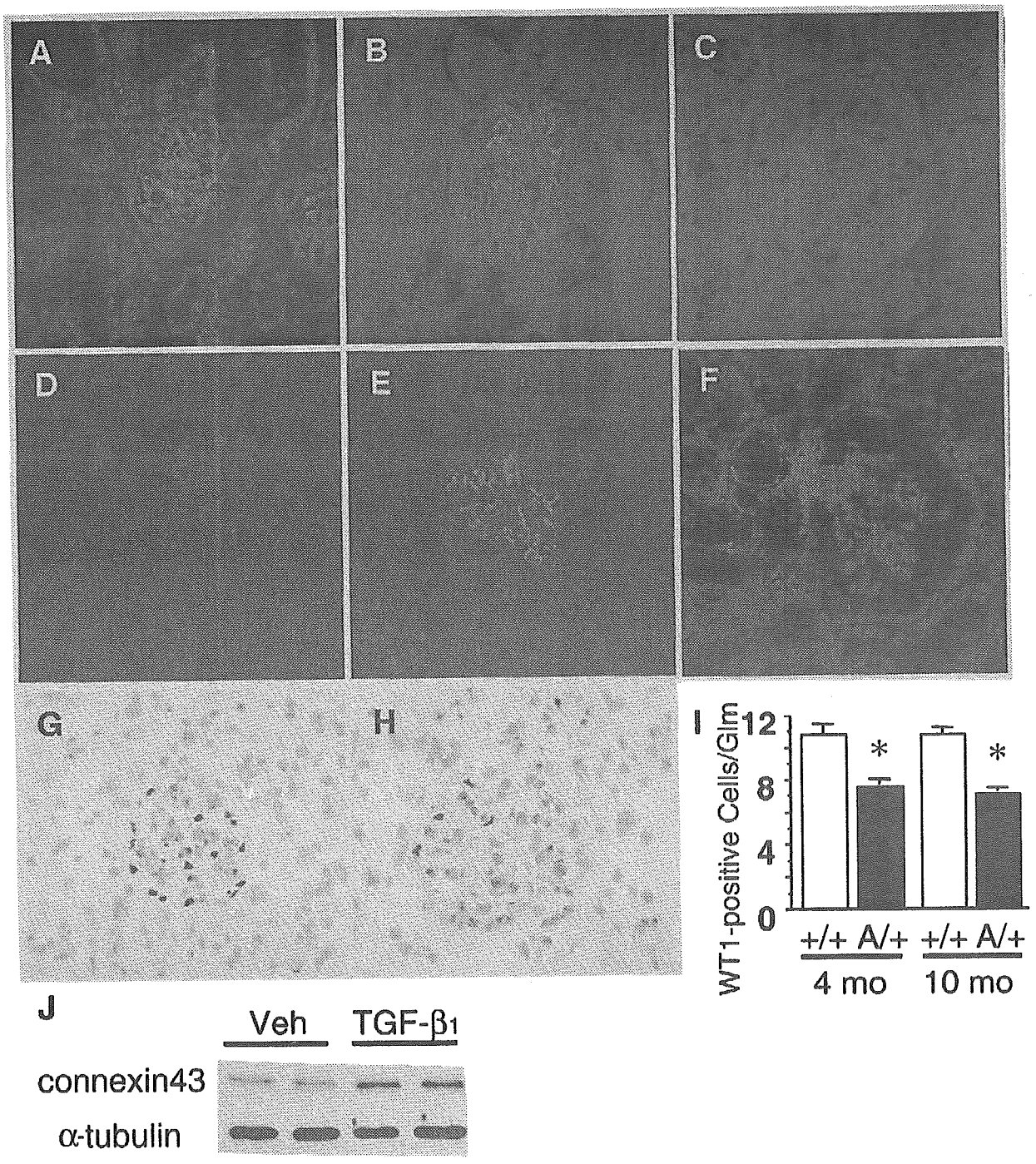

Figure 4. Immunostaining of podocyte markers (nephrin (*A–C*); connexin43 (*D–F*); WT-1 (*G*) and (*H*)) in 4-month-old (*B* and *E*) and 10-month-old (*C*, *F*, and *H*) A-ZIPTg/+ and 10-month-old +/+ (*A*, *D*, and *G*). Linear staining of nephrin along the capillary wall was apparently weak and sparse in 4-month-old A-ZIPTg/+ (*B*), as compared with that in +/+ (*A*), and only faint staining was observed in 10-month-old A-ZIPTg/+ (*C*). Conversely, punctate connexin43 staining along the capillary wall appeared in 4-month-old A-ZIPTg/+ (*E*), although it was observed only in the extraglomerular mesangium in +/+ (*D*). Connexin43 staining was also observed in the mesangial area in 10-month-old A-ZIPTg/+ (*F*). The number of WT-1-positive cells was apparently reduced in glomeruli of A-ZIPTg/+ (*H*) than +/+ (*G*) at 10 months of age. Quantitative analysis showed significant reduction in WT-1-positive cell number in A-ZIPTg/+ as compared with +/+ as early as 4 months of age (*I*). Mean ± SE. A/+; A-ZIPTg/+. *$P < 0.05$, n = 6-11. *J*) Increased protein levels of connexin43 by TGF-β1 treatment in cultured mouse differentiated podocytes.

Fig. 5

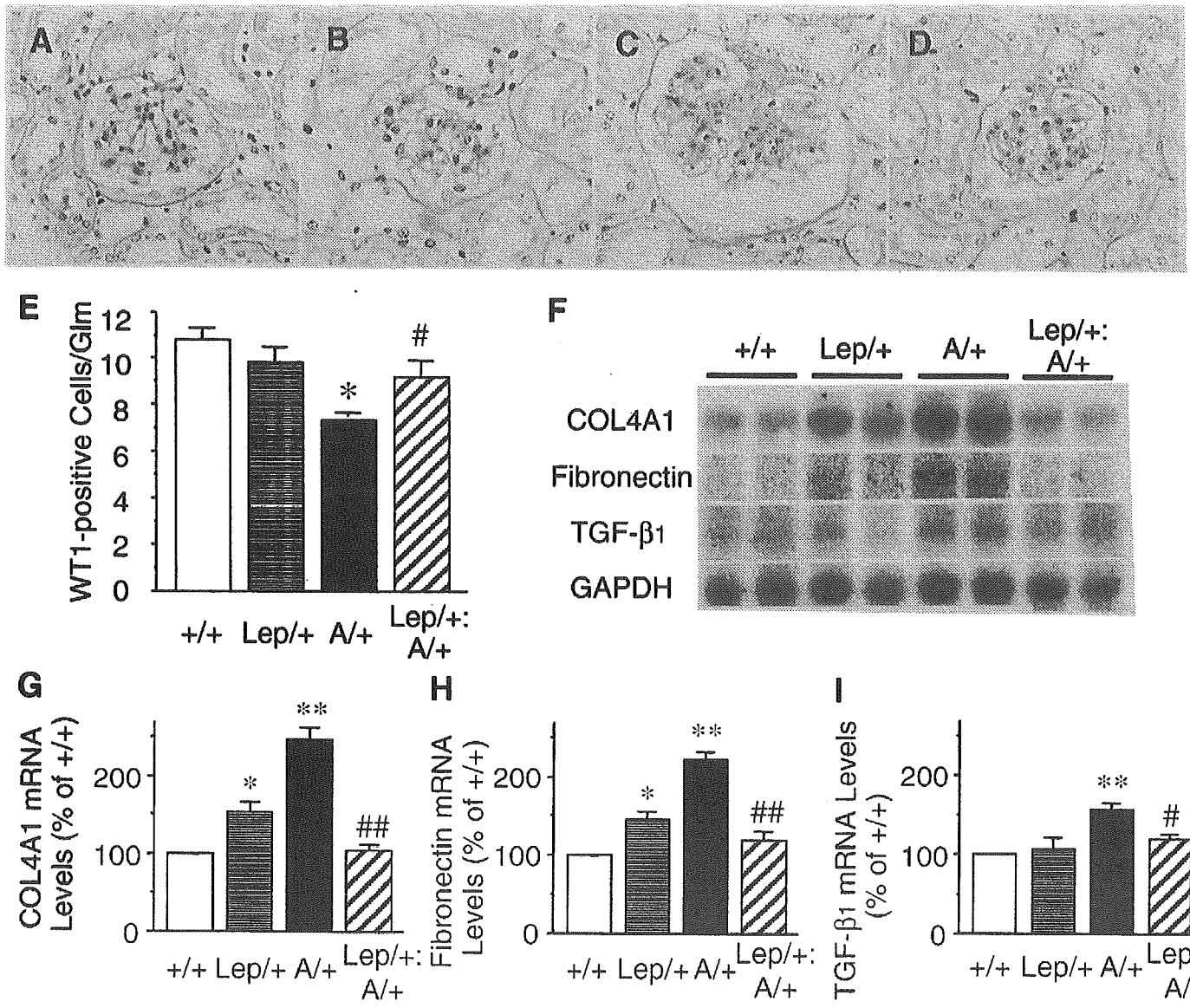

Figure 5. Analysis of 10-month-old F1 mice obtained by crossing A-ZIPTg/+ and LepTg/+. Renal histology of +/+ (*A*), LepTg/+ (*B*), A-ZIPTg/+ (*C*) and LepTg/+:A-ZIPTg/+ (*D*). Periodic acid-Schiff stain, ×400. Reduced number of WT-1-positive cells in A-ZIPTg/+ was also significantly alleviated in LepTg/+:A-ZIPTg/+ (*E*). Renal gene expression of COL4A1, fibronectin, and TGF-β1 in F1 mice (*F–I*). Representative Northern blots (*F*) and quantitative analysis of relative mRNA levels (*G–I*) are shown. Up-regulation of COL4A1, fibronectin, and TGF-β1 gene expression in A-ZIPTg/+ was completely inhibited in LepTg/+:A-ZIPTg/+. Mean ± SE. $*P < 0.05$, $**P < 0.01$ vs. +/+, $\#P < 0.05$, $\#\#P < 0.01$ vs. A-ZIPTg/+, $n = 5–6$.

Fig. 6

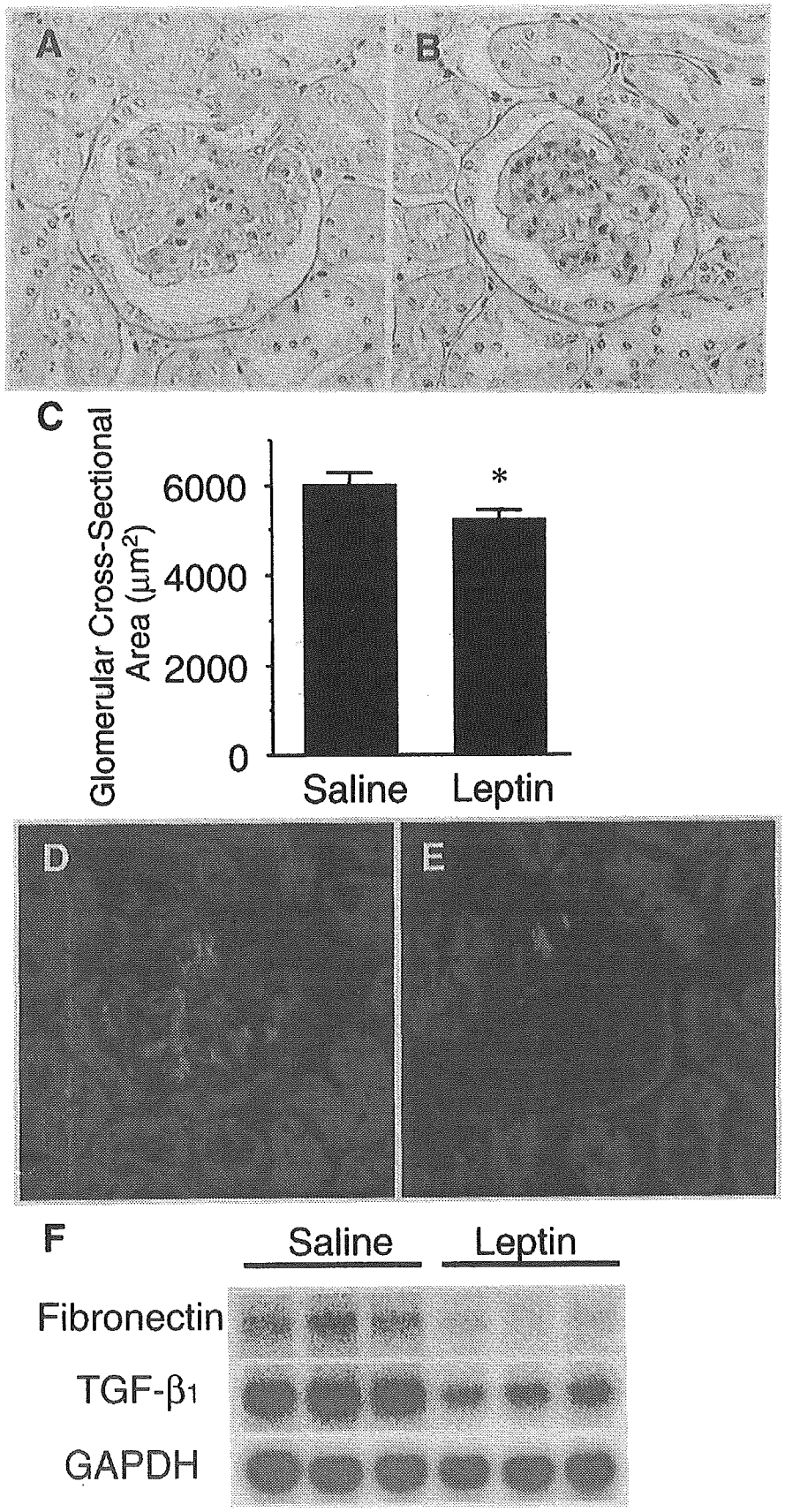
A
B
C
Glomerular Cross-Sectional Area (μm²)
6000
4000
2000
0
*
Saline
Leptin
D
E
F
Saline
Leptin
Fibronectin
TGF-β1
GAPDH

Figure 6. Effects of continuous leptin administration on renal injury in 10-month-old A-ZIPTg/+. Renal histology of leptin-treated (*A*) and saline-treated (*B*) A-ZIPTg/+. Periodic acid-Schiff stain, ×400. Quantitative analysis of glomerular hypertrophy (*C*). Mean ± SE. $^*P < 0.05$ vs. saline-treated A-ZIPTg/+, $n = 7$. Immunofluorescence study of TGF-β1 (*D* and *E*). Leptin-treated A-ZIPTg/+ (*E*) exhibited marked reduction of TGF-β1 staining as compared with saline-treated A-ZIPTg/+ (*D*). Northern blot analysis of TGF-β1 and fibronectin (*F*). Up-regulation of TGF-β1 and fibronectin gene expression was effectively suppressed by continuous leptin treatment.

Available online at www.sciencedirect.com
SCIENCE DIRECT
Journal of Molecular and Cellular Cardiology 38 (2005) 185–192
Journal of Molecular and Cellular Cardiology
www.elsevier.com/locate/yjmcc

Original Article

Hypertrophic responses to cardiotrophin-1 are not mediated by STAT3, but via a MEK5-ERK5 pathway in cultured cardiomyocytes

Nobuki Takahashi [a], Yoshihiko Saito [b,*], Koichiro Kuwahara [a], Masaki Harada [a], Keiji Tanimoto [a], Yasuaki Nakagawa [a], Rika Kawakami [a], Michio Nakanishi [a], Shinji Yasuno [a], Satoru Usami [a], Akihiko Yoshimura [c], Kazuwa Nakao [a]

[a] *Department of Medicine and Clinical Science, Kyoto University Graduate School of Medicine, Kyoto, Japan*
[b] *First Department of Internal Medicine, Nara Medical University, 840 Shijo-cho, Kashihara-city, Nara 634-8522, Japan*
[c] *Division of Molecular and Cellular Immunology, Medical Institute of Bioregulation, Kyushu University, Fukuoka, Japan*

Received 18 June 2004; received in revised form 3 October 2004; accepted 22 October 2004

Available online 10 December 2004

Abstract

gp130-dependent signaling is known to play a critical role in the onset of heart failure. In that regard, cardiotrophin-1 (CT-1) activates several signaling pathways via gp130, and induces hypertrophy in neonatal rat cardiomyocytes. Among the mediators activated by CT-1, STAT3 is thought to be important for induction of cell hypertrophy, though its precise function in the CT-1 signaling pathway is not fully understood. In the present study, therefore, to better understand the significance of STAT3 activity in CT-1 signaling, we infected cultured cardiomyocytes with adenoviral vectors harboring a dominant-negative STAT3 mutant or one of two endogenous negative regulators of cytokine signaling via the Janus kinase (JAK)-signal transducer and activator of transcription (STAT) pathways [suppressor of cytokine signaling (SOCS) 1 and 3] and then examined their effects on three indexes of CT-1-induced cell hypertrophy: protein synthesis, secretion of brain natriuretic peptide and changes in cell surface area. In control cells, CT-1-induced both STAT3 phosphorylation and cell hypertrophy. Overexpression of dominant-negative STAT3 mutant suppressed CT-1-induced STAT3 phosphorylation, but did not affect cell hypertrophy. On the other hand overexpression of SOCS1 or SOCS3 inhibited both CT-1-induced STAT3 phosphorylation and cell hypertrophy. CT-1 also induced phosphorylations of ERK1/2 and ERK5 in cardiomyocytes, and those, too, were suppressed by overexpression of SOCSs. CT-1-induced cell hypertrophy was suppressed by overexpression of a dominant-negative MEK5 mutant, and not by overexpression of a dominant-negative MEK1 mutant. These findings indicate that the major pathway responsible for the hypertrophic responses to CT-1 is not JAK-STAT3 pathway nor MEK1-ERK1/2 pathway, but MEK5-ERK5 pathway.

Keywords: Cardiotrophin-1; Cytokine; ERK1/2; ERK5; STAT3; Cell signaling; Hypertrophy; Cardiomyocyte

1. Introduction

Cardiotrophin-1 (CT-1) is an interleukin-6 (IL-6)-related cytokine that exerts various hypertrophic and antiapoptotic effects via the gp130-leukemia inhibitory factor (LIF) receptor complex by activating several intracellular signaling in cardiomyocytes, including the Janus kinase (JAK)-signal transducer and activator of transcription (STAT) and mitogen-activated protein kinase (MAPK) pathways [1]. The receptors for IL-6-related cytokines share gp130 as a signal-transducing receptor component [1]. Its continuous activation in heart due, for example, to overexpression of IL-6 and its receptor is known to cause myocardial hypertrophy [2]. Conversely, ventricular restricted gp130-deficient mice display massive apoptosis of cardiomyocytes and are unable to achieve compensatory hypertrophy during aortic pressure overload [3]. So it is very important to elucidate the physi-

Abbreviations: BNP, brain natriuretic peptide; CT-1, cardiotrophin-1; ERK, extracellular signal-regulated kinase; ET-1, endothelin-1; GPCR, G-protein-coupled receptor; IL-6, interleukin-6; JAK, Janus kinase; LIF, leukemia inhibitory factor; MAPK, mitogen-activated protein kinase; MEK, MAPK/ERK kinase; PI3K, phosphatidylinositol 3-OH kinase; SOCS, suppressor of cytokine signaling; STAT, signal transducer and activator of transcription.

* Corresponding author. Tel.: +81-744-29-8850; fax: +81-744-22-9726.
E-mail address: yssaito@nmu-gw.naramed-u.ac.jp (Y. Saito).

0022-2828/$ - see front matter © 2004 Elsevier Ltd. All rights reserved.
doi:10.1016/j.yjmcc.2004.10.016

ological or pathophysiological role of IL-6-related cytokines in the heart.

On the other hand, little is known about the significance of the signaling pathways downstream of gp130 that mediates the phenotypic, namely hypertrophic and antiapoptotic effects of IL-6-related cytokines such as CT-1. We previously showed that CT-1 induces its antiapoptotic effects via the phosphatidylinositol 3-OH kinase (PI3K)-Akt pathway [4]. In addition, others have shown that LIF, which shares a receptor with CT-1, induces hypertrophy in cardiomyocytes via STAT3 [5], and that cardiac-specific overexpression of STAT3 leads to myocardial hypertrophy [6]. In those cases, however, the contribution made by STAT3 did not appear especially pronounced, making it unclear whether STAT3 mediated transduction in the principal pathway leading to hypertrophy. In that regard, we have shown that CT-1-induced STAT3 activation leads to upregulation of two endogenous negative regulators of cytokine signaling via JAK-STAT pathways [suppressor of cytokine signaling (SOCS) 1 and 3, also referred to as JAK-binding protein (JAB) and cytokine-inducible SH2 protein (CIS) 3/STAT-induced STAT inhibitor (SSI) 1and 3] [7–9] in the heart [10].

Finally, Kodama et al. [11] have shown that the MAPK/extracellular signal-regulated kinase (ERK) kinase (MEK)1/2-ERK1/2 pathway is critically involved in LIF-induced cardiomyocyte hypertrophy. Moreover, Nicol et al. [12] recently reported that in cardiomyocytes LIF activates ERK5, a novel member of the MAPK family, and that a dominant-negative form of MEK5, the MAPK kinase directly responsible for activation of ERK5, inhibits LIF-induced elongation of cardiomyocytes.

With those as background, we hypothesized that the major molecule responsible for the hypertrophic responses to IL-6-related cytokines may not be STAT3, but ERK1/2 or ERK5. So in this study, we examined the effects of overexpressing SOCSs, dominant-negative mutant of STAT3, MEK1 or MEK5 on CT-1-induced cardiomyocyte hypertrophy with the aim of better understanding the significance of the STAT3 and MEK-ERK pathways in CT-1-induced cardiac hypertrophy.

2. Materials and methods

2.1. Materials

Recombinant rat CT-1 was prepared using a GST-fusion system (Pharmacia Biotechnology, Inc.) according to the manufacturer's instructions. Human endothelin-1 (ET-1) was purchased from Peptide Institute. Anti-STAT3, anti-phospho-STAT3 (Tyr705), anti-p44/42 MAPK (ERK1/2), anti-phospho-ERK1/2 (Thr202/Tyr204) and anti-phospho-ERK5 (Thr218/Tyr220) antibodies were from Cell Signaling Technology. Anti-ERK5/BMK1 antibody was from Upstate Biotechnology. Anti-SOCS3/CIS3 antibody was from Immuno-Biological Laboratories. PD98059 was from Calbiochem.

2.2. Recombinant adenoviruses

Adenoviral vectors harboring the genes for LacZ (Ad-LacZ), myc-tagged SOCS1 (AdSOCS1), myc-tagged SOCS3 (AdSOCS3), an HA-tagged dominant-negative STAT3 mutant (AdSTAT3F) in which phosphorylation-site Tyr705 was substituted with Phe [13], and Cre recombinase (AdCre) were gifts from Dr. Yasushi Hanakawa, Ehime University School of Medicine, Ehime, Japan [14]; an adenoviral vector containing the gene for a dominant-negative MEK5 mutant (AdMEK5KM) in which ATP-binding Lys106 was substituted with Met [15] was a gift from Dr. Eric N. Olson, University of Texas, Dallas, USA [12]; and an adenoviral vector harboring the gene for a dominant-negative MEK1 mutant (AdMEK1DN) in which Asp208 in the kinase subdomain VII was substituted with an Ala [16] was a gift from Dr. Seinosuke Kawashima, Kobe University, Kobe, Japan. Because of the toxic effect of SOCS1 on 293 cells used for recombinant virus production, a Cre-LoxP conditional expression system was employed to generate AdSOCS1 using the protocol described by Kanegae et al. [17]. For that reason, only AdSOCS1 was co-infected with AdCre. All adenoviral vectors harbor the cytomegalovirus enhancer and the chicken β-actin promoter.

2.3. Cardiomyocyte culture and adenovirus infection

Ventricular myocytes were prepared from 1-day-old Wistar rats using a Percoll gradient as previously described [18]. The investigation conforms to the Guiding Principles in the Care and Use of Animals (American Physiological Society). After collecting the myocytes from the gradient, they were preplated on noncoated dishes for 1 h, after which the unattached cells were collected; this cell population consisted of >97% myocytes as assessed by immunofluorescence with anti-rat sarcomeric actin antibody (DAKO Japan Co., Ltd.). The myocytes were then plated on gelatin-coated dishes in serum-containing medium for 24 h. The medium was then replaced with serum-free medium, and the cells were infected for 24 h with one of the recombinant adenoviruses at a multiplicity of infection (MOI) of 10 viral particles per cell. Under these conditions, >99% of the myocytes were infected (assessed by X-gal staining or immunocytochemistry with anti-tag antibodies). Thereafter, the cells were treated with 10^{-9} mol/l CT-1 or 10^{-8} mol/l ET-1 for the indicated times. In some cases, the MEK inhibitor PD98059 was applied for 30 min prior to addition of CT-1 or ET-1.

2.4. Western blot analysis

After incubating the cells with CT-1 or ET-1 for the indicated times, they were washed with ice-cold phosphate-buffered saline (PBS) and lyzed with lysis buffer (Cell Signaling Technology). The resultant whole-cell protein extracts were subjected to 10% SDS-PAGE, and the resolved proteins were electrophoretically transferred onto polyvinylidene dif-

luoride membranes (Bio-Rad Laboratories). The membranes were then blocked with 5% skim milk (Difco Laboratories) and probed with the indicated antibodies.

2.5. Analysis of protein synthesis in cultured cells

Protein synthesis in cultured cardiomyocytes was evaluated using [^{3}H]-leucine incorporation as an index. Following incubation with CT-1 or ET-1, the cells were cultured for 24 h, after which 3 μCi of [^{3}H]-leucine (Amersham Life Science) was added for an additional 24 h. After washing twice with ice-cold PBS, the cells were incubated in 10% trichloroacetic acid for 30 min at 4 °C. The resultant precipitate was solubilized in 0.2 N NaOH for >4 h, and the radioactivity was measured in a liquid scintillation counter.

2.6. Radioimmunoassay for brain natriuretic peptide

Levels of brain natriuretic peptide (BNP) in medium conditioned for 48 h by cardiomyocytes after stimulation with CT-1 or ET-1 was measured using a specific radioimmunoassay as previously described [19].

2.7. Statistical analysis

Data are presented as mean ± standard deviations (S.D.) of results of four independent experiments. Unpaired Student's *t*-tests were used to determine significant differences between two groups, and ANOVA with post hoc Fisher's tests was used to determine significant differences among three or four groups. Values of $P < 0.05$ were considered significant.

3. Results

3.1. Effects of SOCSs and STAT3F on CT-1-induced STAT3 phosphorylation

First, to determine whether SOCSs are the true endogenous negative regulators of CT-1 signaling in our cultured cardiomyocytes, Western blot analysis was carried out using samples from CT-1-treated cardiomyocytes probed with anti-SOCS3 antibody. As shown in Fig. 1A, upregulation of SOCS3 protein was confirmed in CT-1-treated cardiomyocytes. We previously showed that CT-1 induced tyrosine phosphorylation of STAT3 in cardiomyocytes, and that the response peaked within 5–15 min of CT-1 application [20]. Next, therefore, we examined the effects of overexpressing SOCS1, SOCS3 and STAT3F on levels of STAT3 tyrosine phosphorylation after 10 min of CT-1 stimulation. AdSOCS1, AdSOCS3 and AdSTAT3F did not have an influence on the basal phosphorylation of STAT3 (Fig. 1B). As shown in Figs. 1B, and 1C, CT-1 induced substantial phosphorylation of STAT3 in cardiomyocytes infected with AdLacZ. This effect was completely blocked in cardiomyocytes infected with AdSOCS1 or AdSOCS3, and significantly inhibited in

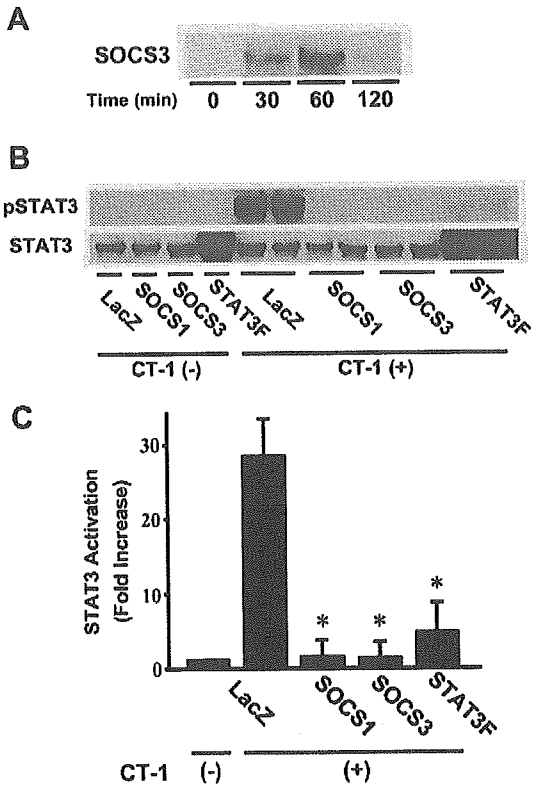

Fig. 1. SOCS3 expression induced by CT-1 and effects of SOCS1, SOCS3 and STAT3F on CT-1-induced phosphorylation of STAT3. (**A**) Representative Western blots showing the time course SOCS3 protein expression in CT-1-treated cardiomyocytes without adenovirus infection. (**B**) Representative Western blots showing the effects of SOCS1, SOCS3 and STAT3F on CT-1-induced phosphorylation of STAT3. Cardiomyocytes infected with AdLacZ, AdSOCS1, AdSOCS3 or AdSTAT3F were treated with 10^{-9} mol/L CT-1 for 10 minutes, after which cell lysates were harvested. (**C**) Phospho-STAT3 (pSTAT3) and STAT3 were measured densitometrically from immunoblots like those in panel B. The ratio of pSTAT3 to STAT3 was normalized to that in AdLacZ-infected cardiomyocytes without CT-1 treatment, which was assigned a value of 1. Only in regard to AdSTAT3F-infected group, the ratio to the average STAT3 of the other adenovirus-infected groups was used. Values are means ± S.D. (n = 8) of four independent experiments, each experiment performed with two distinct samples; *$P < 0.01$ vs. LacZ with CT-1.

cardiomyocytes infected with AdSTAT3F. The apparently augmented expression of STAT3 in cardiomyocytes infected with AdSTAT3F reflects the cross-reaction of anti-STAT3 antibody with overexpressed STAT3F, and is indicative of the efficiency of the protein expression in cardiomyocytes transfected using these recombinant adenoviral vectors.

3.2. Effects of SOCSs and STAT3F on CT-1-induced cardiomyocyte hypertrophy

We next examined the effects of overexpressing SOCS1, SOCS3 or STAT3F on CT-1-induced hypertrophy of cardiomyocytes. For comparison, ET-1, a G-protein-coupled receptor (GPCR) agonist, was also used to induce a distinct form of cardiomyocyte hypertrophy [21]. We first evaluated CT-1- and ET-1-induced [^{3}H]-leucine incorporation as an index of protein synthesis. As shown in Fig. 2A, CT-1 significantly increased [^{3}H]-leucine incorporation in cardiomyocytes

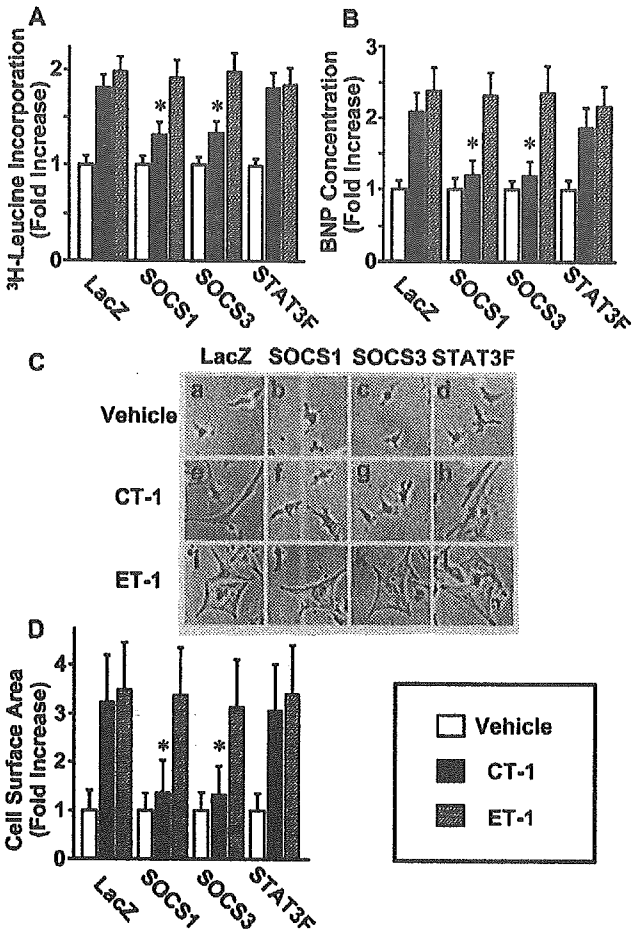

Fig. 2. Effects of SOCS1, SOCS3 and STAT3F on CT-1-induced cardiomyocyte hypertrophy. Cardiomyocytes infected with AdLacZ, AdSOCS1, AdSOCS3 or AdSTAT3F were treated with vehicle (open bars), 10^{-9} mol/L CT-1 (solid bars) or 10^{-8} mol/L ET-1 (hatched bars). The fold increase is relative to vehicle-treated cells of each adenovirus-infected group. (**A**) ^{3}H-leucine incorporation by cardiomyocytes during the period from 24 to 48 hours after treatment. (**B**) BNP concentration in the cultured media 48 hours after treatment. (**C**) Phase-contrast photographs of cultured cardiomyocytes taken 48 hours after treatment with vehicle *(a-d)*, CT-1 *(e-h)* or ET-1 *(i-l)*. (**D**) Cell surface areas were analyzed using NIH Image software. A total of 100 cells were examined for each group. The experiments were repeated four times independently, and each was performed with six distinct samples (**A, B**). Values are means ± S.D. (n = 24 in A and B, n = 100 in D); $^*P < 0.05$ vs. LacZ with CT-1.

infected with AdLacZ. This effect was significantly inhibited by infection with AdSOCS1 or AdSOCS3 but, somewhat surprisingly, not by infection with AdSTAT3F. Infection with AdSOCS1, AdSOCS3 or AdSTAT3F had no effect on ET-1-induced [^{3}H]-leucine incorporation.

The effects of AdSOCS1, AdSOCS3 and AdSTAT3F on BNP secretion from cardiomyocytes paralleled their effects on [^{3}H]-leucine incorporation (Fig. 2B)—i.e. infection with AdSOCS1 or AdSOCS3 significantly inhibited CT-1-induced BNP secretion, whereas infection with AdSTAT3F did not. ET-1-induced BNP secretion was unaffected by AdSOCS1, AdSOCS3 or AdSTAT3F.

CT-1- and ET-1-induced cardiomyocyte hypertrophy was also examined by evaluating their effect on cell shape and surface area. Consistent with an earlier report [21], CT-1 induced a characteristic hypertrophy in cardiomyocytes infected with AdLacZ (Fig. 2Ce)—i.e. it elicited pronounced increases in cell length, but did not significantly affect the width. ET-1, by contrast, elicited increases in both cell length and width (Fig. 2Ci). Infection with AdSOCS1 or AdSOCS3 (Fig. 2Cf, g and 2D), but not AdSTAT3F (Fig. 2Ch and 2D), inhibited CT-1-induced changes in cell shape and size. ET-1-induced changes in cell shape and size were unaffected by AdSOCS1, AdSOCS3 or AdSTAT3F (Fig. 2Cj-l and 2D).

3.3. Effects of SOCSs and STAT3F on CT-1-induced ERK phosphorylation

Collectively, the results presented so far indicate that inhibition of STAT3 alone does not inhibit CT-1-induced cardiomyocyte hypertrophy. Only when SOCSs are used to inhibit other signaling pathways is the hypertrophy inhibited. In that regard, CT-1 is known to also induce activation of ERK1/2 in cardiomyocytes [1], while LIF, another IL-6-related cytokine, has been reported to induce activation of ERK5 in cardiomyocytes [12]. With that in mind, we examined the effects of overexpressing SOCS1, SOCS3 or STAT3F on CT-1-induced activation (phosphorylation) of ERK1/2 and ERK5. AdSOCS1, AdSOCS3 and AdSTAT3F did not affect the basal phosphorylation of ERK1/2 nor ERK5 (Fig. 3D). We found that CT-1-induced phosphorylation of both ERK1/2 and ERK5 that peaked within ~10 min (Fig. 3A–C), and these effects were significantly inhibited by infection with AdSOCS1 or AdSOCS3, but not AdSTAT3F (Fig. 3D–F). Thus, the effects of overexpressing SOCS1, SOCS3 or STAT3F on CT-1-induced ERK activation differed from the effects on STAT3 activation, but paralleled the effects on cardiomyocyte hypertrophy.

3.4. Effects of PD98059 on CT-1-induced ERK phosphorylation and on CT-1-induced cardiomyocyte hypertrophy

The MEK1 inhibitor PD98059 [22] was recently shown to also inhibit MEK5, the specific upstream activator of ERK5, though at a somewhat higher concentration [23]. Likewise, we found that PD98059 concentration-dependently inhibited CT-1-induced phosphorylation of both ERK1/2 and ERK5, but that it was a more potent inhibitor of the former (Fig. 4A–C). PD98059 also inhibited both CT-1- and ET-1-induced [^{3}H]-leucine incorporation and BNP secretion (Fig. 4D, E). It is noteworthy that the potency of the inhibitory effect of PD98059 on the activities of CT-1 and ET-1 paralleled the potency of its effect on the phosphorylation of ERK5 and ERK1/2, respectively.

3.5. Effects of dominant-negative MEK1 and MEK5 mutants on CT-1-induced cardiomyocyte hypertrophy

The results obtained with PD98059 were confirmed when we examined the effects of overexpressing dominant-negative

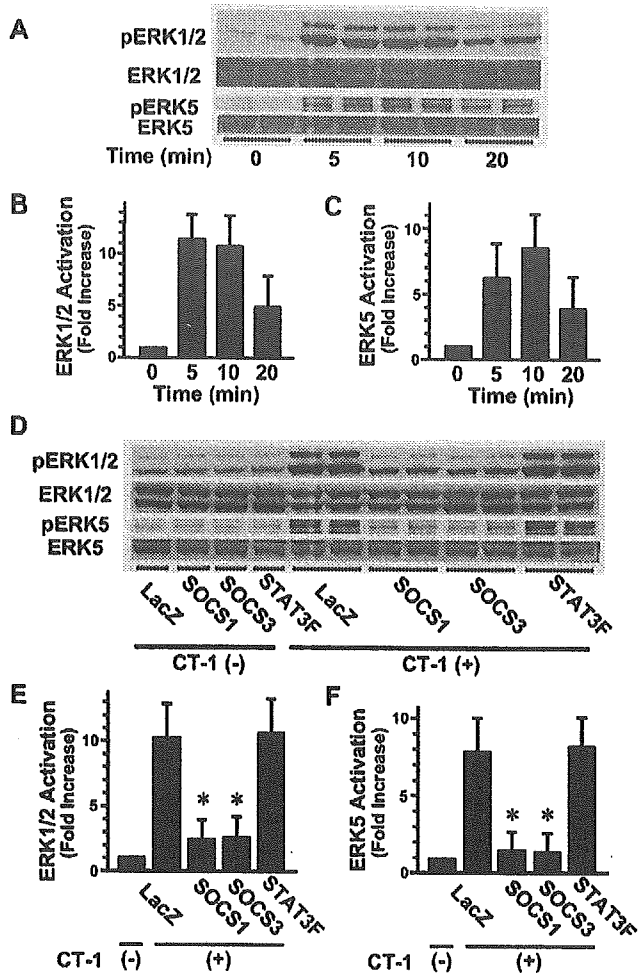

Fig. 3. Time course of CT-1-induced phosphorylation of ERK1/2 and ERK5, and effects of SOCS1, SOCS3 and STAT3F on CT-1-induced phosphorylation of ERK1/2 and ERK5. (A) Representative Western blots showing the time course of CT-1-induced phosphorylation of ERK1/2 and ERK5. Cardiomyocytes infected with AdLacZ were stimulated with 10^{-9} mol/L CT-1 for the indicated times, after which cell lysates were harvested. (B) Phospho-ERK1/2 (pERK1/2) and ERK1/2 were measured densitometrically from immunoblots like those in panel A. The ratio of pERK1/2 to ERK1/2 was normalized to that in cardiomyocytes without CT-1 treatment, which was assigned a value of 1. (C) Phospho-ERK5 (pERK5) and ERK5 were analyzed as panel B. (D) Representative Western blots showing the effects of SOCS1, SOCS3 and STAT3F on CT-1-induced phosphorylation of ERK1/2 and ERK5. Cardiomyocytes infected with AdLacZ, AdSOCS1, AdSOCS3 or AdSTAT3F were treated with 10^{-9} mol/L CT-1 for 10 min, after which the cell lysates were harvested. (E) Phospho-ERK1/2 (pERK1/2) and ERK1/2 were measured densitometrically from immunoblots like those in panel D. The ratio of pERK1/2 to ERK1/2 was normalized to that in AdLacZ-infected cardiomyocytes without CT-1 treatment, which as assigned a value of 1. (F) Phospho-ERK5 (pERK5) and ERK5 were analyzed in the same way as panel E. Values are means ± S.D. (n = 8) of four independent experiments, each experiment performed with two distinct samples; $^{*}P < 0.05$ vs. LacZ with CT-1.

MEK1 or MEK5 mutants on CT-1-induced phosphorylation of ERKs and cardiomyocyte hypertrophy. As shown in Fig. 5, infection with AdMEK1DN inhibited both the basal phosphorylation of ERK1/2 and CT-1-induced phosphorylation of ERK1/2, but did not have an influence on the phosphorylation of ERK5. On the other hand, infection with AdMEK5KM inhibited both the basal phosphorylation of

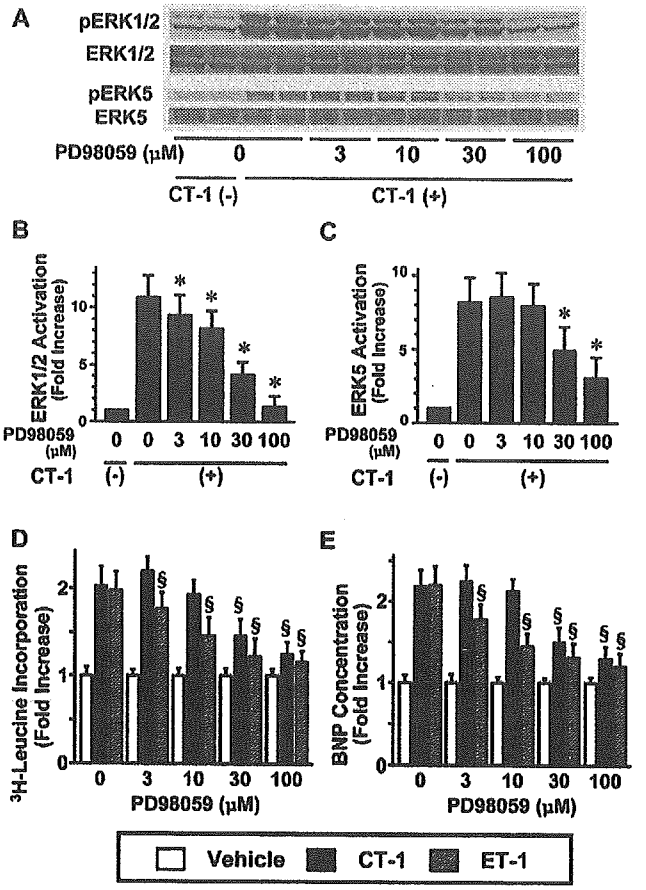

Fig. 4. Effects of PD98059 on CT-1-induced phosphorylation of ERK1/2 and ERK5 and CT-1- and ET-1-induced cardiomyocyte hypertrophy. Cardiomyocytes cultured with the indicated concentration of PD98059 were treated with vehicle (open bars), 10^{-9} mol/L CT-1 (solid bars) or 10^{-8} mol/L ET-1 (hatched bars). (A) Representative Western blots of phospho-ERK1/2 (pERK1/2) and phospho-ERK5 (pERK5) in lysates harvested after 10 minutes of CT-1 treatment. (B) pERK1/2 and ERK1/2 were measured densitometrically from immunoblots like those in panel A. The ratio of pERK1/2 to ERK1/2 was normalized to that in cardiomyocytes without CT-1 treatment, which as assigned a value of 1. (C) pERK5 and ERK5 were analyzed in the same way as panel B. (D) ^{3}H-leucine incorporation by cardiomyocytes during the period from 24 to 48 hours after treatment. (E) BNP concentration in the cultured media 48 hours after treatment. Fold increase is relative to vehicle-treated cells in each concentration group. The experiments were repeated four times independently, and each was performed with two distinct samples (A-C) or with sis distinct samples (D, E). Values are means ± S.D. (n = 8 in A to C, n = 24 in D and E); $^{*}P < 0.05$ vs. PD98059 (-) with CT-1, §$P < 0.05$ vs. LacZ with CT-1 or ET-1, correspondently.

ERK5 and CT-1-induced phosphorylation of ERK5, but did not have an influence on the phosphorylation of ERK1/2. And as shown in Fig. 6, infection with AdMEK5KM but not AdMEK1DN significantly inhibited CT-1-induced increases in [^{3}H]-leucine incorporation, BNP secretion and cell surface area. Conversely, infection with AdMEK1DN but not AdMEK5KM inhibited the ET-1-induced effects.

4. Discussion

The aim of the present study was to assess the significance of the STAT3 and MEK-ERK pathways in CT-1-induced

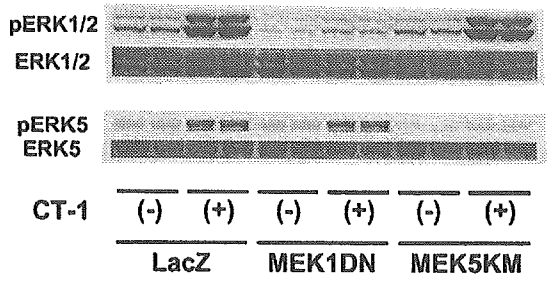

Fig. 5. Effects of dominant-negative MEK1 (MEK1DN) and MEK5 (MEK5KM) mutants on CT-1-induced phosphorylation of ERK1/2 and ERK5. Representative Western blots of phospho-ERK1/2 (pERK1/2) and phospho-ERK5 (pERK5) in lysates harvested after 10 minutes of CT-1 treatment.

hypertrophy of cultured neonatal rat ventricular myocytes. Among several pathways activated by IL-6-related cytokines in cardiomyocytes, the STAT3 pathway is reportedly important for mediating cardiomyocyte hypertrophy [5,6,24]. In our study, however, a dominant-negative STAT3 mutant did not inhibit CT-1-induced cardiomyocyte hypertrophy, although it suppressed activation (phosphorylation) of STAT3. We can not explain strictly the discrepancy of our results from previous study [5], but we think that it may be attributable to the difference of culture conditions, for example the degree of fibroblasts contamination. We have confirmed the existence of STAT3 in cardiac fibroblasts and its phosphorylation induced by CT-1 (data not shown). With the results in our study, the major pathway leading from CT-1 binding to the gp130 complex to cardiomyocyte hypertrophy is not via STAT3. On the other hand, two recently identified [7–9] endogenous negative regulators of cytokine signaling via JAK-STAT pathways, SOCS1 and SOCS3, significantly inhibited both STAT3 phosphorylation and the hypertrophic effects of CT-1, which is consistent with an earlier report [14]. In addition, SOCS1/3 and dominant-negative STAT3 mutant had the same influence on the hypertrophic effects of LIF, another member of IL-6-related cytokines (data not shown), indicating that these differential effects of SOCSs vs. dominant-negative STAT3 are not CT-1 specific, but shared with other members of IL-6-related cytokines. The key question then was what gp130-dependent signaling pathway do SOCSs suppress to inhibit CT-1-induced hypertrophy?

Among the possibilities are the STAT1 pathway [25], the PI3K-Akt pathway [26] and the MEK1/2-ERK1/2 pathway [11,16], all of which appear to be involved in LIF-induced cardiomyocyte hypertrophy. The first two are easily ruled out. We found that dominant-negative STAT3 inhibited CT-1-induced phosphorylation of not only STAT3 but also STAT1 (data not shown), most likely because STAT3 and STAT1 share docking sites for JAK1/2 [1]. Therefore, if CT-1 acted via STAT1, we would expect its effects to have been inhibited by the dominant-negative STAT3 mutant. As for the PI3K-Akt pathway, we previously showed that this pathway is largely responsible for CT-1's antiapoptotic effects rather than cell hypertrophy [4].

This leaves the MEK-ERK pathways. PD98059 is known as a specific inhibitor of MEK1 [22], but some reports suggest that it also inhibits MEK5 at a somewhat higher concentration [23,27]. Consistent with those results, we found that at concentrations <30 μM PD98059 selectively inhibits evoked ERK1/2 phosphorylation and ET-1-induced cardiomyocyte hypertrophy. At concentrations ≥30 μM, however, PD98059 also inhibits ERK5 phosphorylation and CT-1-induced cardiomyocyte hypertrophy. On the other hand, it is also known that PD98059 loses specificity at the higher concentrations. So we added the examinations with dominant-negative MEK1 or MEK5 mutant to confirm our hypothesis acquired from the examinations with PD98059. Dominant-negative MEK1 mutant partially inhibited ET-1-induced hypertrophy, but had not effect on CT-1-induced hypertro-

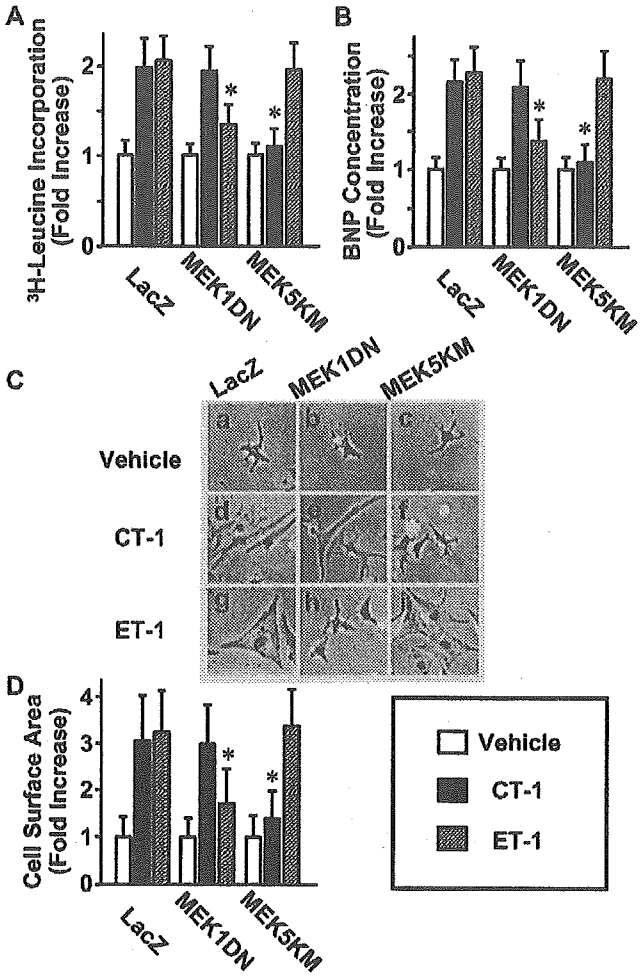

Fig. 6. Effects of dominant-negative MEK1 (MEK1DN) and MEK5 (MEK5KM) mutants on CT-1-induced cardiomyocyte hypertrophy. Cardiomyocytes infected with AdLacZ, AdMEK1DN or AdMEK5KM were treated with vehicle (open bars), 10^{-9} mol/L CT-1 (solid bars) or 10^{-8} mol/L ET-1 (hatched bars). The fold increase is relative to vehicle-treated cells in each adenovirus-infected group. (**A**) ^{3}H-leucine incorporation by cardiomyocytes during the period from 24 to 48 hours after treatment. (**B**) BNP concentration in the cultured media 48 hours after treatment. (**C**) Phase-contrast photographs of cultured cardiomyocytes obtained 48 hours after treatment with vehicle *(a-c)*, CT-1 *(d-f)* or ET-1 *(g-i)*. (**D**) Cell surface areas were analyzed using NIH Image software. A total of 100 cells were examined for each group. The experiments were repeated four times independently, and each was performed with six distinct samples (**A, B**). Values are means ± S.D. (n = 24 in A and B, n = 100 in D); *$P < 0.05$ vs. LacZ with CT-1.

phy, whereas dominant-negative MEK5 mutant almost completely inhibited CT-1-induced hypertrophy, but had no effect on ET-1-induced hypertrophy. We therefore conclude that CT-1-induced cardiomyocyte hypertrophy is mediated mainly via a MEK5-ERK5 pathway, while ET-1-induced hypertrophy is at least partially via a MEK1/2-ERK1/2 pathway. The fact that SOCSs inhibited CT-1-induced phosphorylation of ERK5 indicates they suppress hypertrophic responses to CT-1 through inhibition of a MEK5-ERK5 pathway. These conclusions are further supported by the findings that gp130-deficient [28] and ERK5-deficient mice [29] show similar embryonic cardiovascular defects, suggesting ERK5 is an important mediator situated downstream of gp130 during cardiovascular development.

CT-1-induced cardiomyocyte hypertrophy is distinct from that induced by GPCR agonists including ET-1 and angiotensin II [21]. Pathophysiological significance of GPCR agonists in the heart is undoubted because of the clinical usefulness of angiotensin-converting-enzyme (ACE) inhibitors [30–33]. On the other hand, there is little clinical evidence concerning IL-6-related cytokines including CT-1. With regard to mouse models, however, IL-6-related cytokines are known to induce concentric hypertrophy via gp130 in in vivo heart [2]. Although here we have shown the significance of the MEK5-ERK5 pathway in cardiomyocyte hypertrophy induced by CT-1, a member of IL-6-related cytokines, activated MEK5 has been shown to induce eccentric, not concentric, hypertrophy in in vivo heart [12]. That is to say, activation of only a MEK5-ERK5 pathway can not account for the cardiac phenotype induced by IL-6-related cytokines. Several signaling pathways including JAK-STATs, MEK-ERKs and PI3K-Akt pathways probably cooperate and express the cardiac phenotype induced by IL-6-related cytokines. So it is necessary to investigate more detailed role of not only a MEK5-ERK5 pathway, but also the other signaling pathways downstream of gp130 in the cardiomyocyte or in the heart stimulated with IL-6-related cytokines. Furthermore, it is expected to elucidate the clinical significance of IL-6-related cytokines in the heart.

Finally, our finding that the MEK5-ERK5 pathway plays a critical role in CT-1-induced cardiomyocyte hypertrophy raises the question, what is the role of STAT3 in cardiomyocytes? Kunisada et al. [6] reported that STAT3 transduces a protective signal against doxorubicin-induced cardiomyopathy, but we detected no related phenotypes in cardiomyocytes overexpressing a dominant-negative STAT3 mutant. It may be that the key role played by STAT3 in cardiomyocytes involves the induction of SOCSs [10] and subsequent inhibition of the MEK5-ERK5 pathway.

Acknowledgments

This work was supported in part by research grants from the Japanese Ministry of Education, Culture, Sports, Science and Technology, the Japanese Ministry of Health, Labor and Welfare, and the Research for the Future Program of the Japan Society for the Promotion of Science (JSPS-RFTF96I00204 and 98L00801), and by grants from the Japanese Cardiovascular Research Foundation, Uehara Memorial Foundation and the Smoking Research Foundation. We thank Dr. E. Olson, Dr. S. Kawashima and Dr. Y. Hanakawa for providing adenovirus vectors and thanks to K. Okamura for her excellent secretarial work.

References

[1] Wollert KC, Chien KR. Cardiotrophin-1 and the role of gp130-dependent signaling pathways in cardiac growth and development. J Mol Med 1997;75:492–501.

[2] Hirota H, Yoshida K, Kishimoto T, Taga T. Continuous activation of gp130, a signal-transducing receptor component for interleukin 6-related cytokines, causes myocardial hypertrophy in mice. Proc Natl Acad Sci USA 1995;92:4862–8.

[3] Hirota H, Chen J, Betz UA, Rajewsky K, Gu Y, Ross Jr. J, et al. Loss of a gp130 cardiac muscle cell survival pathway is a critical event in the onset of heart failure during biomechanical stress. Cell 1999;97:189–98.

[4] Kuwahara K, Saito Y, Kishimoto I, Miyamoto Y, Harada M, Ogawa E, et al. Cardiotrophin-1 phosphorylates akt and BAD, and prolongs cell survival via a PI3K-dependent pathway in cardiac myocytes. J Mol Cell Cardiol 2000;32:1385–94.

[5] Kunisada K, Tone E, Fujio Y, Matsui H, Yamauchi-Takihara K, Kishimoto T. Activation of gp130 transduces hypertrophic signals via STAT3 in cardiac myocytes. Circulation 1998;98:346–52.

[6] Kunisada K, Negoro S, Tone E, Funamoto M, Osugi T, Yamada S, et al. Signal transducer and activator of transcription 3 in the heart transduces not only a hypertrophic signal but a protective signal against doxorubicin-induced cardiomyopathy. Proc Natl Acad Sci USA 2000;97:315–9.

[7] Starr R, Willson TA, Viney EM, Murray LJ, Rayner JR, Jenkins BJ, et al. A family of cytokine-inducible inhibitors of signalling. Nature 1997;387:917–21.

[8] Endo TA, Masuhara M, Yokouchi M, Suzuki R, Sakamoto H, Mitsui K, et al. A new protein containing a SH2 domain that inhibits JAK kinases. Nature 1997;387:921–4.

[9] Naka T, Narazaki M, Hirata M, Matsumoto T, Minamoto S, Aono A, et al. Structure and function of a new STAT-induced STAT inhibitor. Nature 1997;387:924–9.

[10] Hamanaka I, Saito Y, Yasukawa H, Kishimoto I, Kuwahara K, Miyamoto Y, et al. Induction of JAB/SOCS-1/SSI-1 and CIS3/SOCS-3/SSI-3 is involved in gp130 resistance in cardiovascular system in rat treated with cardiotrophin-1 in vivo. Circ Res 2001;88:727–32.

[11] Kodama H, Fukuda K, Pan J, Sano M, Takahashi T, Kato T, et al. Significance of ERK cascade compared with JAK/STAT and PI3-K pathway in gp130-mediated cardiac hypertrophy. Am J Physiol Heart Circ Physiol 2000;279:H1635–H1644.

[12] Nicol RL, Frey N, Pearson G, Cobb M, Richardson J, Olson EN. Activated MEK5 induces serial assembly of sarcomeres and eccentric cardiac hypertrophy. EMBO J 2001;20:2757–67.

[13] Minami M, Inoue M, Wei S, Takeda K, Matsumoto M, Kishimoto T, et al. STAT3 activation is a critical step in gp130-mediated terminal differentiation and growth arrest of a myeloid cell line. Proc Natl Acad Sci USA 1996;93:3963–6.

[14] Yasukawa H, Hoshijima M, Gu Y, Nakamura T, Pradervand S, Hanada T, et al. Suppressor of cytokine signaling-3 is a biomechanical stress-inducible gene that suppresses gp130-mediated cardiac myocyte hypertrophy and survival pathways. J Clin Invest 2001;108:1459–67.

[15] English JM, Pearson G, Hockenberry T, Shivakumar L, White MA, Cobb MH. Contribution of the ERK5/MEK5 pathway to Ras/Raf signaling and growth control. J Biol Chem 1999;274:31588–92.

[16] Ueyama T, Kawashima S, Sakoda T, Rikitake Y, Ishida T, Kawai M, et al. Requirement of activation of the extracellular signal-regulated kinase cascade in myocardial cell hypertrophy. J Mol Cell Cardiol 2000;32:947–60.

[17] Kanegae Y, Lee G, Sato Y, Tanaka M, Nakai M, Sakaki T, et al. Efficient gene activation in mammalian cells by using recombinant adenovirus expressing site-specific Cre recombinase. Nucleic Acids Res 1995;23:3816–21.

[18] Harada M, Itoh H, Nakagawa O, Ogawa Y, Miyamoto Y, Kuwahara K, et al. Significance of ventricular myocytes and nonmyocytes interaction during cardiocyte hypertrophy: evidence for endothelin-1 as a paracrine hypertrophic factor from cardiac nonmyocytes. Circulation 1997;96:3737–44.

[19] Nakao K, Ogawa Y, Suga S, Imura H. Molecular biology and biochemistry of the natriuretic peptide system. I: natriuretic peptides. J Hypertens 1992;10:907–9012.

[20] Kuwahara K, Saito Y, Harada M, Ishikawa M, Ogawa E, Miyamoto Y, et al. Involvement of cardiotrophin-1 in cardiac myocyte–nonmyocyte interactions during hypertrophy of rat cardiac myocytes in vitro. Circulation 1999;100:1116–24.

[21] Wollert KC, Taga T, Saito M, Narazaki M, Kishimoto T, Glembotski CC, et al. Cardiotrophin-1 activates a distinct form of cardiac muscle cell hypertrophy. Assembly of sarcomeric units in series VIA gp130/leukemia inhibitory factor receptor-dependent pathways. J Biol Chem 1996;271:9535–45.

[22] Alessi DR, Cuenda A, Cohen P, Dudley DT, Saltiel AR. PD 098059 is a specific inhibitor of the activation of mitogen-activated protein kinase kinase in vitro and in vivo. J Biol Chem 1995;270:27489–94.

[23] Kamakura S, Moriguchi T, Nishida E. Activation of the protein kinase ERK5/BMK1 by receptor tyrosine kinases. Identification and characterization of a signaling pathway to the nucleus. J Biol Chem 1999; 274:26563–71.

[24] Railson JE, Liao Z, Brar BK, Buddle JC, Pennica D, Stephanou A, et al. Cardiotrophin-1 and urocortin cause protection by the same pathway and hypertrophy via distinct pathways in cardiac myocytes. Cytokine 2002;17:243–53.

[25] Kodama H, Fukuda K, Pan J, Makino S, Baba A, Hori S, et al. Leukemia inhibitory factor, a potent cardiac hypertrophic cytokine, activates the JAK/STAT pathway in rat cardiomyocytes. Circ Res 1997;81:656–63.

[26] Oh H, Fujio Y, Kunisada K, Hirota H, Matsui H, Kishimoto T, et al. Activation of phosphatidylinositol 3-kinase through glycoprotein 130 induces protein kinase B and p70 S6 kinase phosphorylation in cardiac myocytes. J Biol Chem 1998;273:9703–10.

[27] Mody N, Leitch J, Armstrong C, Dixon J, Cohen P. Effects of MAP kinase cascade inhibitors on the MKK5/ERK5 pathway. FEBS Lett 2001;502:21–4.

[28] Yoshida K, Taga T, Saito M, Suematsu S, Kumanogoh A, Tanaka T, et al. Targeted disruption of gp130, a common signal transducer for the interleukin 6 family of cytokines, leads to myocardial and hematological disorders. Proc Natl Acad Sci USA 1996;93:407–11.

[29] Regan CP, Li W, Boucher DM, Spatz S, Su MS, Kuida K. Erk5 null mice display multiple extraembryonic vascular and embryonic cardiovascular defects. Proc Natl Acad Sci USA 2002;99:9248–53.

[30] The CONSENSUS Trial Study Group. Effects of enalapril on mortality in severe congestive heart failure. Results of the Cooperative North Scandinavian Enalapril Survival Study (CONSENSUS). N Engl J Med 1987;316:1429–35.

[31] The SOLVD Investigators. Effect of enalapril on survival in patients with reduced left ventricular ejection fractions and congestive heart failure. N Engl J Med 1991;325:293–302.

[32] Swedberg K, Held P, Kjekshus J, Rasmussen K, Ryden L, Wedel H. Effects of the early administration of enalapril on mortality in patients with acute myocardial infarction. Results of the Cooperative New Scandinavian Enalapril Survival Study II (CONSENSUS II). N Engl J Med 1992;327:678–84.

[33] The SOLVD Investigators. Effect of enalapril on mortality and the development of heart failure in asymptomatic patients with reduced left ventricular ejection fractions. N Engl J Med 1992;327:685–91.

ELSEVIER

Bone 36 (2005) 1056 – 1064

BONE

www.elsevier.com/locate/bone

Complementary antagonistic actions between C-type natriuretic peptide and the MAPK pathway through FGFR-3 in ATDC5 cells

Ami Ozasa[a], Yasato Komatsu[a,*], Akihiro Yasoda[a], Masako Miura[a], Yoko Sakuma[a], Yuko Nakatsuru[a], Hiroshi Arai[a], Nobuyuki Itoh[b], Kazuwa Nakao[a]

[a]*Department of Medicine and Clinical Science, Kyoto University Graduate School of Medicine, 54 Shogoin Kawahara-cho Sakyo-ku, Kyoto 606-8507, Japan*
[b]*Department of Genetic Biochemistry, Kyoto University Graduate School of Pharmaceutical Sciences, Japan*

Received 30 September 2004; revised 10 February 2005; accepted 7 March 2005

Abstract

We previously reported that C-type natriuretic peptide (CNP) stimulates endochondral ossification and corrects the reduction in body length of achondroplasia model mouse with constitutive active fibroblast growth factor receptor 3 (FGFR-3). In order to examine the interaction between CNP and FGFR-3, we studied intracellular signaling by using ATDC5 cells, a mouse chondrogenic cell line, and found that FGF2 and FGF18 markedly reduced CNP-dependent intracellular cGMP production, and that these effects were attenuated by MAPK inhibitors. Western blot analysis demonstrated that the level of GC-B, a particulate guanylyl cyclase specific for CNP, was not changed by treatment with FGFs. Conversely, CNP and 8-bromo-cGMP strongly and dose-dependently inhibited the induction of ERK phosphorylation by FGF2 and FGF18 without changing the level of FGFR-3, although they did not affect the phosphorylation of STAT-1. In the organ-cultured fetal mouse tibias, CNP and FGF18 counteracted on the longitudinal bone growth, and both the size and number of hypertrophic chondrocytes. The FGF/FGFR-3 pathway is known as the negative regulator of endochondral ossification. We found that FGFs inhibited CNP-stimulated cGMP production by disrupting the signaling pathway through GC-B while CNP antagonized the activation of the MAPK cascade by FGFs. These results suggest that the CNP/GC-B pathway plays an important role in growth plate chondrocytes and constitutes the negative cross talk between FGFs and the activity of MAPK. Our results may explain one of the molecular mechanisms of the growth stimulating action of CNP and suggest that activation of the CNP/GC-B pathway may be effective as a novel therapeutic strategy for achondroplasia.

Keywords: Natriuretic peptide; Guanylyl cyclase; Chondrocyte; FGF; MAPK

Introduction

The natriuretic peptide family consists of three structurally related peptides: atrial natriuretic peptide (ANP), brain natriuretic peptide (BNP) and C-type natriuretic peptide (CNP) [1]. They can influence a variety of homeostatic processes by accumulation of the intracellular guanosine 3′, 5′-cyclic monophosphate (cGMP) through two subtypes of particulate guanylyl cyclase (GC), GC-A for ANP and BNP, and GC-B for CNP [2]. In skeletal tissues, we have demonstrated that CNP is a positive growth regulator of long bones formed through endochondral ossification via the GC-B/cGMP pathway [3,4]. CNP-depleted mice are characterized by short stature with a phenotype histologically similar that of achondroplasia [3], while the growth plates of explanted long bones in the presence of CNP show a similar histological picture to that of the growth plate cartilage of fibroblast growth factor receptor 3 (FGFR-3)-depleted mice [5]. This raises the possibility that activation of the CNP/GC-B pathway of endochondral bone regulation reverses the inhibitory effect of FGFR-3 signaling in skeletogenesis.

FGFR-3 belongs to a class of tyrosine kinase receptors involved in signal transduction. In the presence of soluble or

* Corresponding author. Fax: +81 75 771 9452.
E-mail address: komatsuy@barium.rirc.kyoto-u.ac.jp (Y. Komatsu).

8756-3282/$ - see front matter © 2005 Elsevier Inc. All rights reserved.
doi:10.1016/j.bone.2005.03.006

cell-surface heparin sulfate proteoglycans, fibroblast growth factors (FGFs) binding to FGFRs induce receptor dimerization and autophosphorylation on tyrosine residues. This then triggers cell proliferation or differentiation through the Ras-Raf-dependent and phospholipase C-dependent signal transduction pathways involving MAPK stimulation [6]. FGFR-3 mutations have been shown to be responsible for achondroplasia, hypochondroplasia and thanatophoric dysphasia (TDI and TDII) [7,8]. These mutations activate receptor signaling by either inducing ligand-independent receptor dimerization or easing the constraints on autophosphorylation of receptor-tyrosine kinase [9]. It has recently been reported that, of the 23 members of the FGF family, FGF-18 is a physiologic ligand for FGFR-3 in chondrocytes and plays an important role as a mediator in skeletal development [10–12].

To gain further insight into the cellular basis of the interaction between CNP and FGFs in endochondral bone formation, we used ATDC5 cells, which constitute a mouse chondrogenic cell line derived from embryogenic carcinoma cells [13]. In the presence of insulin, these cells differentiate into chondrocytes, form cartilage nodules, serially exhibit several differentiation markers for the chondrocytes, and are eventually mineralized, thus reflecting the endochondral ossification process in vivo. We previously demonstrated that ATDC5 cells contain particularly high activity levels for GC-B and also appear to contain low levels of GC-A and the soluble form of guanylyl cyclase, which is responsive to nitric oxide [14]. Therefore, ATDC5 cells are considered to be a good model to study the interaction between CNP and FGFs in vitro.

We also studied the effects of CNP and FGF18 on organ-cultured fetal mouse tibias. Since the growth plates consist of several zones, each representing a different stage of differentiation and functioning differently, the interaction between the cells in the different zones can be crucial for a given substance to exert its effects. We previously developed an ex vivo organ culture system of mouse long bones [4]. During a 5-day culture, the bones exhibited longitudinal growth mostly due to the growth in the cartilage primordial rather than the ossified portion. This system was therefore considered a good ex vivo model for studying the interaction between CNP and FGFs. The purpose of the study presented here was to clarify the interaction between the CNP/GC-B pathway and FGF signaling in growth plate chondrocytes, as well as the mechanism of this interaction, in order to determine the efficacy of activation of CNP/GC-B as a novel therapeutic strategy for achondroplasia.

Materials and methods

Human C-type natriuretic peptide was purchased from Peptide Institute, Inc. (Minoh, Japan), 8-bromo cGMP and isobutylmethylxanthine (IBMX) from Sigma-Aldrich Co. (St. Louis, MO, USA), and human recombinant FGF2 from Pepro Tech EC. Ltd. (London, England). Rat recombinant FGF18 was generously provided by Amgen Inc. (Thousand Oaks, CA, USA). Primary antibodies, rabbit anti-phospho-ERK1/2 antibodies, rabbit anti- ERK1/2 antibodies, and anti-STAT-1 antibodies were obtained from Cell Signaling Technology Inc. (Beverly, MA, USA), rabbit anti-phospho-STAT-1 antibodies from Upstate Biotechnology, (Lake Placid, NY, USA), and HRP-conjugated donkey anti-rabbit IgG antibodies from Amersham Pharmacia Biotech, (Freiburg, Germany). The MEK (MAPK-ERK kinase) inhibitors U0126 and PD098059 were purchased from Cell Signaling Technology Inc., fetal calf serum (FCS) was purchased from Sankou Junyaku (Tokyo, Japan), and Ham F12/DMEM 50/50 medium and Bigger's BJG medium were obtained from GIBCO (Grand Island, NY, USA).

Cell culture conditions

Cells were grown and maintained using standard techniques. ATDC5 cells were maintained in Ham F12/DMEM 50/50 medium containing 5% FCS, antibiotics, and insulin (10 ng/ml). Confluent cells were maintained for 14 days and considered quiescent after maintenance in 0.5% FCS for 24 h. For radioimmunoassay, cells were seeded on 24-multiwell culture plates, and on a 6 cm dish (BD Bioscience, NJ, USA) for Western blotting and real-time PCR analysis.

Intracellular cGMP determination

Quiescent cells were treated with FGFs for 1 h. The cells were then preincubated in Ham F12/DMEM 50/50 medium containing 0.5% FCS and 1 mM IBMX at room temperature for 10 min. CNP was added at a concentration of 10^{-9}–10^{-7} M and incubated at 37°C for 30 min in the presence of 1 mM IBMX. Reactions were terminated immediately by aspirating the medium, washing the cells with ice-cold PBS, and freezing them in 500 μl of 50 mM HCl. The acidified extracts were analyzed for guanylyl cyclase activity. The level of cGMP was determined by radioimmunoassay after succinylation (Yamasa Co. Ltd., Chosi, Chiba, Japan). To examine the effect of FGFs, we also used the MEK inhibitors U0126 and PD098059, which were added 1 h before treatment of CNP. The level of cGMP was determined as already described.

Western blot analysis

Quiescent cells were incubated with a medium containing CNP (10^{-7}–10^{-6} M) or 10^{-4} M 8-bromo cGMP for 1 h. The medium was then switched to an FGF-containing one, and the cells were treated with FGFs (10 ng/ml) for 3 min. Cells were extracted with the aid of a solvent solution (0.5 M Tris–HCl, 10% SDS, β-mercaptoethanol, glycerol, and Bromo-phenol blue). Soluble proteins were electrophoretically resolved on 8% acrylamide, 0.1% SDS gels and

transferred to polyvinylidene fluoride membranes (Immobilon-P; Millipore, Billerica, MA, USA). The membranes were probed overnight with antibodies against phosphorylated ERK1/2, ERK1/2, phosphorylated STAT-1 or STAT-1, according to the supplier's instructions. The membranes were then probed with secondary antibodies for 1 h. Bound antibodies were detected by chemiluminescence (ECL, Amersham Pharmacia Biotech, Piscataway, NJ, USA) and their density measured by using the public domain National Institute of Health IMAGE program.

The expression of GC-B in ATDC5 cells was analyzed by Western blot analysis. Quiescent cells were incubated with a medium containing FGF18 (1 or 10 ng/ml) for 1 h, after which the cells were extracted and the proteins blotted to the membrane as described above. The membranes were probed for 1 h with the rabbit polyclonal anti-GC-B antibody [15] (a generous gift from Dr. D.L. Garbers of the University of Texas Southwestern Medical Center) and bound antibodies were detected as described above.

To confirm the effect of the MEK inhibitor on phosphorylated ERK1/2, we used 20 μM U0126, and the MEK inhibitor (U0126) was added 1 h before treatment of FGF2.

Real-time PCR analysis of FGFR-3

Quiescent cells were incubated with a medium containing CNP (10^{-6} M) for 1 h and total RNAs were extracted using ISOGEN (Nippon Gene Co. Ltd., Toyama, Japan) according to the manufacturer's instructions. After synthesis of the first-strand cDNA from 1 μg of total RNA by means of Superscript II RT (Life Technologies, Inc., St. Louis, MO, USA) with random hexamers, Taqman-PCR was performed with the ABI Prism 7700 sequence detection system and Taqman Universal PCR Mastermix (Applied Biosystems, Foster City, CA, USA) using FAM and VIC-labeled fluorogenic probes specific for FGFR-3 or the internal standard 18 S rRNA. All samples were run in duplicate in 96-well plates in the ABI Prism 7700 sequence. There was no significant difference in 18 S rRNA levels among experimental groups.

Organ culture of embryonic mouse tibias

Organ culture of fetal mouse tibias was performed with the suspension culture technique in a chemically defined medium (Bigger's BJG medium). Tibial explants from 16-day-old normal ICR mouse embryos were cultured for 5 days with or without 10 ng/ml FGF18 and 10^{-7} M CNP. After a 5-day culture, the total bone length was measured longitudinally by using a linear ocular scale mounted on an inverted microscope. Explants were fixed in 4% paraformaldehyde, decalcified in 10% EDTA/0.1 M Tris–HCl, pH 7.4, for 7 days, and embedded in paraffin. 5-μm-thick sections cut from the paraffin-embedded specimens were stained with Alcian blue (pH 2.5) and hematoxylin/eosin (H&E).

Immunohistochemical staining for type X collagen, using a polyclonal rabbit anti-type X collagen antibody (1:5000; LSL, Tokyo, Japan) as a primary antibody, was also performed. Immunoreactions were visualized by using a biotinylated antipolyvalent antibody, a streptavidin–biotin–horseradish peroxidase complex, and diaminobenzidine (Vector Laboratories, Inc., Burlingame, CA, USA). The specificity of the immunoreactions was controlled by omitting the primary antibody.

The size of hypertrophic cells was measured on 5-μm-thick sections of cultured tibias with a computerized measurement system (KS400 Imaging System; Carl Zeiss, Eching, Germany), and the cells of hypertrophic chondrocytes were manually counted.

Statistical analysis

Data are expressed as the mean ± SE. The changes in cGMP were compared by means of ANOVA using Fisher's test. Comparisons between groups of organ cultured bone lengths were performed with the unpaired *t* test. Probabilities less than 0.05 were considered statistically significant.

Results

Inhibition by FGF2 of CNP signaling in ATDC5 cells

ATDC5 cells were differentiated into chondrocytes for a 14-day culture after confluency [13], and we confirmed that collagen type X, a marker of hypertrophic chondrocytes, was expressed in these cells [16]. In ATDC5 cells, CNP (10^{-9}–10^{-7} M) stimulated the production of intracellular cGMP in a dose-dependent manner with a 36-fold increase of the basal level at 10^{-7} M CNP (55 ± 3 fmol/well to 1985 ± 181 fmol/well). This increase was inhibited up to 53% by the addition of 10 ng/ml of FGF2 (1045 ± 65 fmol/well) (Fig. 1A). Pretreatment with U0126, a specific inhibitor of the upstream of ERK (MEK) [17], at a concentration of 20 μM partially undid the reduction of cGMP by FGF2 (1395 ± 144 fmol/well vs. 1980 ± 143 fmol/well) compared with the vehicle (Fig. 1B). The same level of recovery was observed after pretreatment with another MEK inhibitor, PD098059, also at a concentration of 20 μM (1425 ± 276 fmol/well vs. 1620 ± 206 fmol/well). Western blot analysis was performed to confirm the blockade of U0126 to ERK1/2 phosphorylation by FGF2. Pretreatment with 20 μM U0126 completely blocked the phosphorylation of ERK1/2 (Fig. 1B inset).

Inhibition by FGF18 of CNP signaling in ATDC5 cells

We analyzed the effect of FGF18, the specific ligand for FGFR-3 in chondrocytes, on CNP-dependent cGMP production in ATDC5 cells. As in the case of FGF2, FGF18 inhibited intracellular cGMP production in ATDC5 cells in a dose-dependent manner (0.3–100 ng/ml). Preincubation

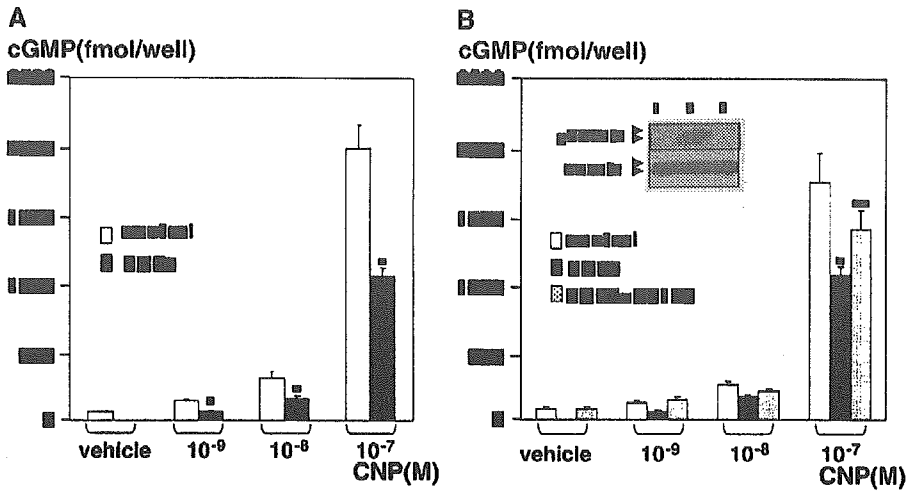

Fig. 1. Inhibition by FGF2 of CNP signaling in ATDC5 cells. The effects of FGF2 on CNP-dependent cGMP production in ATDC5 cells. (A) Controls (open columns) show CNP stimulation of the intracellular cGMP production in a dose-dependent manner (10^{-9}–10^{-7} M CNP), and this increase was inhibited by pretreatment with 10 ng/ml FGF2 (closed columns). Columns represent means ± SE (n = 6, each), *P < 0.01 vs. control (B) MEK inhibitor, U0126 (dotted columns) resulted in recovery from the reduction of cGMP by 10 ng/ml FGF2 (closed columns). Columns represent means ± SE (n = 6, each), *P < 0.01 vs. control (DMSO 0.0025%) (open columns), **P < 0.01 vs. FGF2. Inset, 20 μM U0126 completely blocked the phosphorylation of ERK1/2 in ATDC5 cells. 1: Control (DMSO 0.0025%), 2: treatment with 10 ng/ml FGF2, 3: pretreatment with 20 μM U0126.

with 3 ng/ml FGF18 significantly inhibited the increase in 10^{-7} M CNP stimulated cGMP production (1425 ± 82 fmol/well vs. 1975 ± 111 fmol/well). This inhibition by FGF18 reached 64% at a concentration of 10 ng/ml and 100 ng/ml FGF18 (1255 ± 11 fmol/well) (Fig. 2).

No effect of FGF18 on GC-B expression in ATDC5 cells

To confirm the expression level of GC-B, the specific receptor for CNP in ATDC5 cells, we performed Western blot analysis using antiserum specific for GC-B. The quiescent ATDC5 cells expressed a certain amount of GC-B at 120-kDa band, which incubation with FGF18 (1 or 10 ng/ml) for 1 h did not alter (Fig. 2 inset).

Attenuation by CNP of MAPK activity of FGFs

The effect of CNP on the downstream signaling of FGFR-3 in ATDC5 cells was analyzed next. ERK1/2 phosphorylation was barely detectable at the basal level but was noticeably stimulated with the addition of FGF2 (10 ng/ml) and FGF18 (10 ng/ml) in ATDC5 cells. Treatment of quiescent ATDC5 cells with CNP (10^{-7}–10^{-6} M) for 1 h prior to the addition of FGF2 and FGF18 reduced the phosphorylation of ERK1/2 in a dose-dependent manner. 10^{-6} M CNP completely eliminated the FGF-stimulated phosphorylation of ERK1/2 (Figs. 3A, B), while 10^{-4} M 8-bromo cGMP also inhibited ERK1/2 phosphorylation of FGF2 (Fig. 3C).

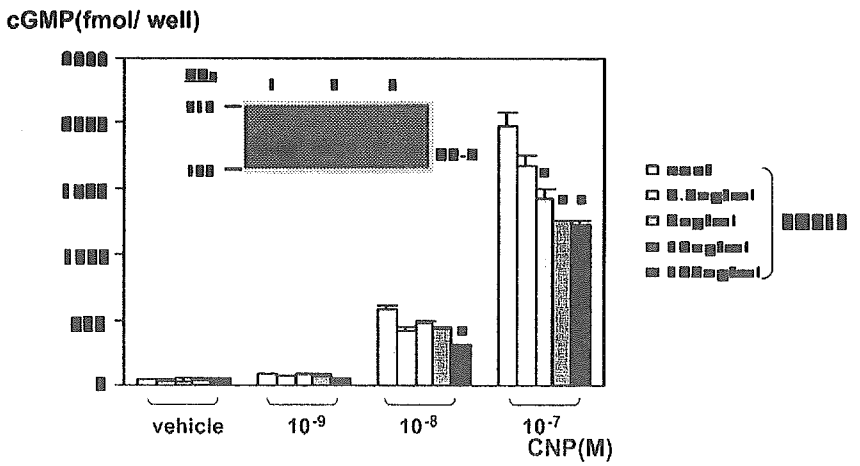

Fig. 2. Inhibition by FGF18 of CNP signaling in ATDC5 cells. The effects of FGF18 on CNP-dependent cGMP production in ATDC5 cells. As in the case of FGF2, FGF18 inhibited the increase in CNP induced cGMP in a dose-dependent manner (0.3–100 ng/ml). Columns represent means ± SE (n = 6, each), *P < 0.01 vs. control. Inset, expression of GC-B in ATDC5 cells (Western blot analysis). 1: Vehicle, 2: treatment with 1 ng/ml FGF18, 3: treatment with 10 ng/ml FGF18.